



## ORIGINAL ARTICLE

# Determination of the solubility of rivaroxaban (anticoagulant drug, for the treatment and prevention of blood clotting) in supercritical carbon dioxide: Experimental data and correlations



Gholamhossein Sodeifian\*, Mohammad Mahdi Behvand Usefi,  
Fariba Razmimanesh, Armin Roshanghias

Department of Chemical Engineering, Faculty of Engineering, University of Kashan, 87317-53153 Kashan, Iran  
Laboratory of Supercritical Fluids and Nanotechnology, University of Kashan, 87317-53153 Kashan, Iran  
Modeling and Simulation Centre, Faculty of Engineering, University of Kashan, 87317-53153 Kashan, Iran

Received 23 July 2022; accepted 9 November 2022  
Available online 16 November 2022

## KEYWORDS

Supercritical carbon dioxide;  
Rivaroxaban;  
Solubility;  
Peng-Robinson;  
Sodeifian model;  
Soave-Redlich-Kwong

**Abstract** Supercritical processes are utilized in pharmaceutical, chemical, agricultural and food industries. To design the micro or nanoparticles formation processes via a supercritical fluid (SCF), it is necessary to have available the solubility data of a solid solute in a solvent such as supercritical carbon dioxide (SC-CO<sub>2</sub>). In this article, the solubility of rivaroxaban (anticoagulant drug, for the treatment and prevention of blood clotting) in SC-CO<sub>2</sub> was investigated for the first time. Six semi-empirical models (Chrastil, Bartle, Jouyban, Garlapati and Madras, and Sodeifian) and two equation of states (EoSs) including Peng-Robinson (PR) and Soave-Redlich-Kwong (SRK) with twin-parametric van der Waals (vdW2) and covolume dependent (CVD) mixing rules were used to examine the correlation of drug solubility data. The best performance was obtained by semi-empirical Jouyban model (Average absolute relative deviation (AARD) = 12.436 %) and PR-vdW2 EoS (AARD = 5.104 %). Total and vaporization enthalpies were calculated 43.617 KJ.mol<sup>-1</sup> and 63.288 KJ.mol<sup>-1</sup>, respectively.

© 2022 The Authors. Published by Elsevier B.V. on behalf of King Saud University. This is an open access article under the CC BY-NC-ND license (<http://creativecommons.org/licenses/by-nc-nd/4.0/>).

\* Corresponding author.

E-mail address: [sodeifian@kashanu.ac.ir](mailto:sodeifian@kashanu.ac.ir) (G. Sodeifian).

Peer review under responsibility of King Saud University.



## Nomenclature

$a_0$ - $a_7$	Parameters for density-based models	$S$	Solubility of rivaroxaban in equilibrium state (g/L)
$a, b$	EoS constants	SRK	Soave-Redlich-Kwong
AARD%	Percent of average absolute relative deviation	SSE	Sum of squares error
$C_s$	Concentration of drug inside collection vial ( $\mu\text{g}/\text{mL}$ )	$SS_R$	Regression sum of squares
CVD	Covolume dependent mixing rule	$SS_T$	Total sum of squares
$H_{\text{sol}}$	Rivaroxaban solvation heat in kJ/mol	SCF	Supercritical fluid
$H_{\text{sub}}$	Rivaroxaban vaporization heat in kJ/mol	SC-CO <sub>2</sub>	Supercritical carbon dioxide
$H_{\text{tot}}$	Total enthalpy of rivaroxaban in kJ/mol	$T$	Temperature (K)
$K_{12}$ & $l_{12}$	Interaction parameters of Eqs. (19) and (20)	$T_b$	Boiling temperature (K)
$M_{ij}$	Interaction parameters of Eqs. (27) and (28)	$T_r$	Reduced temperature
$M_{\text{CO}_2}, M_s$	Molar mass of CO <sub>2</sub> , and drug in g/mol	$T_c$	Critical temperature (K)
$MS_R$	Mean square regression	$U$	Expanded uncertainty
$MS_E$	Mean square residual	$V_s$	Molar volume of rivaroxaban drug ( $\text{cm}^3/\text{mol}$ )
$n_{\text{CO}_2}$	Mole of CO <sub>2</sub>	$V_S(L)$	Volumes of the collection vial
$n_{\text{solute}}$	Mole of rivaroxaban drug	$V_I(L)$	Volume of the sampling loop
$N$	The number of experimental data	vdW2	Twin-parametric van der Waals mixing rule
NIST	National Institute of Standards and Technology	$y_2$	Equilibrium molar fraction
$P$	Pressure (bar)	$y_i^{\text{calc}}$	Calculated values of the solute solubility
$P_c$	Critical pressure (bar)	$y_i^{\text{exp}}$	Experimental value of the solute solubility
$P_{\text{ref}}$	Reference pressure (0.1 MPa)	<i>Greek Symbols</i>	
$P_{\text{sub}}$	Pure solid sublimation pressure (Pa)	$\rho_{\text{CO}_2}, \rho_1$	Density of SC-CO <sub>2</sub> ( $\text{kg}/\text{m}^3$ )
PR	Peng – Robinson	$\omega$	Acentric factor
$Q$	Number of independent variables in each equation		
$R$	Universal gas constant in J/(mol · K)		
$R^2$	Correlation coefficient		

## 1. Introduction

Rivaroxaban is an oral, direct Factor Xa inhibitor, which is at an advanced stage of clinical development for prevention and treatment of thromboembolic disorders (Mueck et al., 2011). In fact, this anticoagulant drug can be used for the treatment and prevention of blood clotting. It was also evaluated for auxiliary anticipation after intense coronary disorder (Mega et al., 2012) and for thromboprophylaxis in intensely sick therapeutic patients (Cohen et al., 2011; Douxfils et al., 2012). The bioavailability of drugs after consumption depend on their solubility and solubility rate in an aqueous medium. For improvement these essential properties, the particle size reduction is an important tool (Sodeifian et al., 2020). Traditional methods for reducing particle size in the pharmaceutical industry include milling, evaporation, recrystallization, etc. (Sodeifian et al., 2017; Adachi and Lu, 1983). For this purpose, a supercritical fluid (SCF) process is useful in the pharmaceutical and biochemical industries compared to conventional methods. SCFs have properties between gas and liquid, such as viscosity, density and diffusivity, providing a wide application range for energy, solubility, polymers, extraction and etc. (Brunner, 2015; Sim Yeoh et al., 2013; Kiran, 2016; Sodeifian et al., 2020).

In general, using SCF technology, morphology, shape, and size of particles can be changed, which increases the efficiency and performance of the drug (Sodeifian et al., 2021). The common methods used in SCF technology can be mentioned RESS, SAS, GAS, RESOLVE ASES, SEDS, SFEE and PGSS

(Chen et al., 2018; Montes et al., 2017; Jafari et al., 2015; Ciou et al., 2018; Lee et al., 2020; Kodama et al., 2018; Lee et al., 2018; Banchemo, 2021; Aredo et al., 2021; Tokunaga et al., 2021; Razmimanesh et al., 2021). This is attributed to the supercritical conditions, as stated before, where properties of CO<sub>2</sub> are between gas and liquid. This provides a suitable situation for CO<sub>2</sub> solvent to achieve particle formation. Supercritical carbon dioxide (SC-CO<sub>2</sub>), widely used as a solvent, is one of the most common SCFs and it has a low critical temperature (304 K) and pressure (73.8 bar). Other characteristics of SC-CO<sub>2</sub> include non-toxic, non-flammable, good chemical stability, inert, recyclable and low cost (Sodeifian et al., 2016; Sodeifian et al., 2018; Shamsipur et al., 2004; Sodeifian and Sajadian, 2017; Taberner et al., 2012; Nasri, 2018; Coelho et al., 2016). To design and optimize drug processes such as micro/nanoparticles of drug particles, knowing the solubility of drug compounds in SCF is essential (Sang et al., 2017; Chen et al., 2017; Sodeifian et al., 2020).

Due to the experimental limitations like time consuming and high cost of experiments in various temperatures and pressures to measure the solubility of a drug in SC-CO<sub>2</sub>, the use of semi-empirical methods and mathematical modeling is valuable tools to investigate the solubility behavior (Hazaveie et al., 2020; Jouyban et al., 2005; Bartle et al., 1991). There are various methods for modeling and correlation of solubility data, which can be referred to EoSs with different mixing rules, semi-empirical models, solubility models and artificial neural networks (ANN) (Nasri, 2018; Huang et al., 2013; Sodeifian et al., 2020). For modeling solubility data using EoS, it is

related to phase equilibria and thermodynamic properties. EoS-based models require a knowledge of physico-chemical properties of solid (drug). In the most cases, these properties are not available for pharmaceuticals and can be used group contribution methods to calculate them (Sodeifian et al., 2017; Farrokh-Niae et al., 2008; Yazdizadeh et al., 2011). Some of the common mixing rules are vdW1, vdW2, Kwak-Mansoori and Wong-Sandler. Furthermore, semi-empirical models are simpler than EoSs and only need temperature, pressure, and density of SC-CO<sub>2</sub>. These models do not require an additional information of solutes (Sim Yeoh et al., 2013; Garlapati and Madras, 2009; Jouyban et al., 2005; Hozhabr et al., 2014). In this work, semi-empirical models with different adjustable parameters from three to six such as Chrastil (Bian et al., 2016); Bian et al. (Bian et al., 2015); Khansary et al. (Asgarpour Khansary et al., 2015); Spark et al. (Sparks et al., 2008); Jouyban et al. (Jouyban et al., 2002), and Sodeifian et al. (Sodeifian et al., 2021) models were applied to compare the accuracy of models for correlating the experimental solubility data.

To the best of knowledge, there is no yet any report on the measurement and modeling of rivaroxaban drug in SC-CO<sub>2</sub>. Accordingly, for the first time, the solubility of rivaroxaban was measured in various temperatures (308–338 K) and pressures (120–270 bar). Then the solubility data was investigated and correlated by different EoSs (PR and SRK) (Sheikhi-Kouhsar et al., 2015; Jaubert and Privat, 2010) with twin-parametric van der Waals (vdW2) (Esmailzadeh et al., 2009) and covolume dependent (CVD) (Yazdizadeh et al., 2012) mixing rules; and with six semi-empirical equations based on density. The used models were evaluated by statistical analysis. Finally, total and vaporization enthalpies were estimated in SC-CO<sub>2</sub> for the first time.

## 2. Experimental

### 2.1. Materials

Methanol was purchased from Merck company (Germany). Pure CO<sub>2</sub> (99.99 %) was provided by Fadak company (Kashan, Iran). Rivaroxaban with formulation C<sub>19</sub>H<sub>18</sub>ClN<sub>3</sub>O<sub>5</sub>S (molar mass = 435.90 g/mol) was prepared by Parsian company (Tehran, Iran). Some properties of the used materials are shown in Table 1.

### 2.2. Experimental details

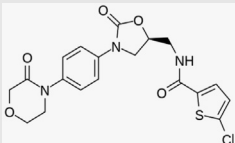
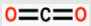
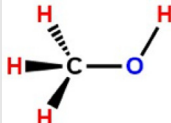
Experimental set up for measuring the solubility of rivaroxaban is shown in Fig. 1 (Sodeifian et al., 2019). Previous articles can be used to know more details (Sodeifian et al., 2021; Sodeifian et al., 2020).

Components used include a CO<sub>2</sub> storage cylinder, a refrigerator, a filter, a solubility column, a sample collector, and temperature and pressure measuring equipment. First, the refrigerator turned on and the temperature was set at 253 K. After the refrigerator temperature was stabilized, the CO<sub>2</sub> in the tank was directed to the refrigerator. CO<sub>2</sub> gas liquefied at 253 K. Liquid CO<sub>2</sub> entered the reciprocating pump (Haskel model, MS-110, 0.33HP, air-driven liquid pump, USA) with the pressure in the tank (about 60 bar) to provide the desired pressure. Then fixed with a barometer up to ±1 bar (U(p) = 1 bar). To maintain the experimental temperatures at the desired levels, a temperature-controlled oven with a temperature accuracy of  $u(T) = 0.1$  K was utilized. A 70 mL equilibrium vessel (cell), containing glass beads of 2 mm in diameter and sintered filters (1 μm) on its both sides filled with 0.5 g of rivaroxaban drug for all experimental data, was placed in an oven to ensure that its temperature remains within ± 0.1 K. The cell was then saturated with high-pressure CO<sub>2</sub> for 60 min to reach the equilibrium state that was determined by varying the contact times (Fig. 1S). After equilibrium, a 2-status 6-way port valve collected 600 μL of saturated SC-CO<sub>2</sub> and added it to a vial with 4 mL methanol. As a final step, the loop was washed with the solvent (1 mL) and the final volume of the solution was adjusted to 5 mL. Rivaroxaban absorbance in methanol was measured with a spectrophotometer, UNICO-4802 UV-Vis at  $\lambda^{\max}$ . The solubility tests were performed three times to determine averages. At the end of the experiments, 100 μg of the drug was dissolved in methanol. A number of standard solutions were then produced by diluting the initial solution to draw the calibration curve. The equilibrium molar fraction ( $y_2$ ), and solubility (S) at different temperatures and pressures in SC-CO<sub>2</sub> were calculated as follows:

$$y_2 = \frac{n_{\text{Solute}}}{n_{\text{solute}} + n_{\text{CO}_2}} \quad (1)$$

Two parameters  $n_{\text{Solute}}$  and  $n_{\text{CO}_2}$  are moles of solute (drug) and CO<sub>2</sub>, respectively that:

**Table 1** Some properties of the used materials.

Compound	Structure	M <sub>w</sub> (g/mol)	CAS number	Melting point	Purity (mass%) and purification method by supplier
Rivaroxaban		435.90	366789-02-8	230 °C	≤99.99, HPLC
Carbon dioxide		44.01	124-38-9		≥99.99, GC
Methanol		32.04	67-56-1		99.98, GC

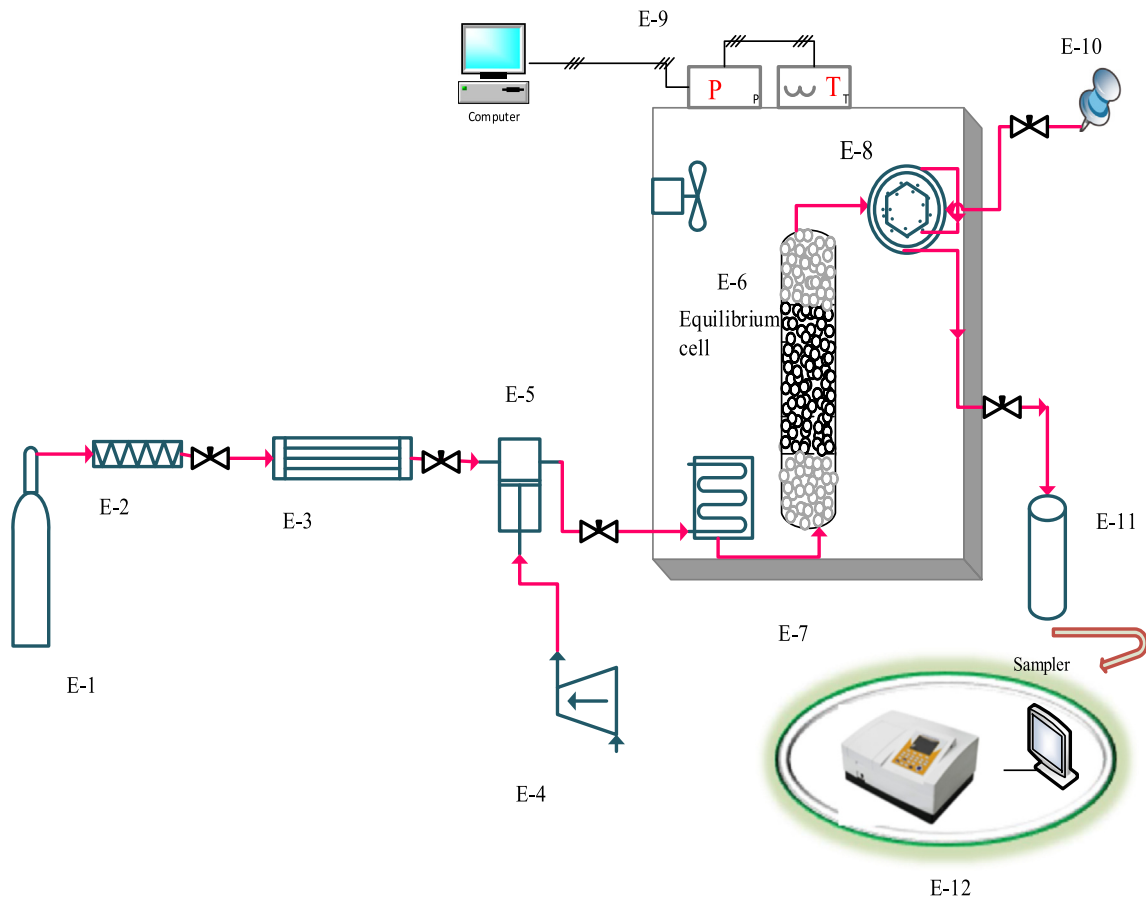


**Fig. 1** Schematic of experimental process. E-1 CO<sub>2</sub> cylinder; E-2, filter; E-3, refrigerator unit; E-4, air compressor; E-5, high pressure pump (Haskel model, MS-110, 0.33HP, air-driven liquid pump, USA); E-6, equilibrium cell; E-7, oven; E-8, six-port, two position valve (injection ring); E-9, control panel; E-10, syringe; E-11, collection vial; E-12, spectrophotometer UV-vis.

$$n_{\text{Solute}} = \frac{C_S \left(\frac{\text{g}}{\text{L}}\right) \cdot V_S(\text{L})}{M_S \left(\frac{\text{g}}{\text{mol}}\right)} \quad (2)$$

$$n_{\text{CO}_2} = \frac{V_l(\text{L}) \cdot \rho \left(\frac{\text{g}}{\text{L}}\right)}{M_{\text{CO}_2} \left(\frac{\text{g}}{\text{mol}}\right)} \quad (3)$$

$M_S$  and  $M_{\text{CO}_2}$  are molecular weight of solute and CO<sub>2</sub>, respectively.

And

$$S \left(\frac{\text{g}}{\text{L}}\right) = \frac{C_S \left(\frac{\text{g}}{\text{L}}\right) \cdot V_S(\text{L})}{V_l(\text{L})} \quad (4)$$

$C_S$  is the solute concentration in the collection vial,  $V_S(\text{L})$  is volume of the collection vial ( $5 \times 10^{-3}$ ),  $V_l(\text{L})$  is volume of the sampling loop ( $600 \times 10^{-6}$ ). The expanded uncertainty of experimental solubility data is presented in Table 3.

### 3. Thermodynamic framework

To investigate the correlation of solubility of rivaroxaban in SC-CO<sub>2</sub>, the two EoSs (PR and SRK) with vdW2 and CVD mixing rules and six semi-empirical models based on density were used.

#### 3.1. Semi-empirical models

In this paper, six semi-empirical were used to investigate the correlation of rivaroxaban solubility in SC-CO<sub>2</sub>. Two models of Chrastil and Belghait, relating a solute solubility to density and temperature of SCF, and other models including Sodeifian, Jouyban, Bartle and Jafari Nejad, relating solubility to temperature, pressure and density of SCF, were used. Table 2 shows the equations of these models.

#### 3.2. Equation of state (EoS) models and mixing rules

The following formula is used to calculate the solubility of rivaroxaban in SC-CO<sub>2</sub>, assuming that SC-CO<sub>2</sub> and rivaroxaban are compound 1 and 2, respectively:

$$y_2 = \frac{P_2^{\text{sub}}(T)}{P} \frac{\phi_2^{\text{sat}}}{\phi_2(T, P, Y)} \exp \left[ \frac{v_2^s (P - P_2^{\text{sub}}(T))}{RT} \right] \quad (5)$$

$P_2^{\text{sub}}(T)$  is sublimation pressure of drug,  $\phi_2^{\text{sat}}$  is saturation fugacity coefficient of the solute,  $\phi_2$  is fugacity coefficient of the solute in supercritical phase and  $v_2^s$  is solid molar volume. If  $P^{\text{sub}}$  is very small, assuming that the saturation pressure of

**Table 2** Representation of semi-empirical models equation used in this work.

Model	Equation	Number of parameters	References
Chrastil	$\ln S = a_0 \ln \rho + \frac{a_1}{T} + a_2$	3	(Sridar et al., 2013)
Bartle	$\ln\left(\frac{y_2 P}{P_{ref}}\right) = a_0 + \frac{a_1}{T} + a_2 (\rho - \rho_{ref})$	3	(Reddy and Garlapati, 2019)
Jafari Nejad	$\ln y_2 = a_0 + a_1 P^2 + a_2 T^2 + a_3 \ln \rho$	4	(Jafari Nejad et al., 2010)
Jouyban	$\ln y_2 = a_0 + a_1 \rho + a_2 P^2 + a_3 PT + \frac{a_4 T}{P} + a_5 \ln \rho$	6	(Si-Moussa et al., 2017)
Sodeifian	$\ln(y_2) = a_0 + \frac{a_1 P^2}{T} + a_2 \ln(\rho_1 T) + a_3(\rho_1 \ln(\rho_1)) + a_4 P \ln(T) + a_5 \frac{\ln(\rho_1)}{T}$	6	(Sodeifian et al., 2019)
Belghait	$\ln y_2 = a_0 + a_1 \rho_{CO_2} + a_2 \rho_{CO_2}^2 + a_3 \rho_{CO_2} T + a_4 T + a_5 T^2 + a_6 \ln \rho_{CO_2} + \frac{a_7}{T}$	8	(Belghait et al., 2018)

**Table 3** Solubility of rivaroxaban (component 2) in SC-CO<sub>2</sub>(component 1). The relative combined standard uncertainty and the

experimental standard deviation expanded uncertainty are  $S(y_k) = \sqrt{\frac{\sum_{j=1}^n (y_j - \bar{y})^2}{n-1}}$ ,  $U = k * u_{combined}$  and  $u_{combined}/y = \sqrt{\sum_{i=1}^N (P_i u(x_i)/x_i)^2}$

Temperature (K) <sup>a</sup>	Pressure (bar) <sup>a</sup>	Density of SC-CO <sub>2</sub> (kg.m <sup>-3</sup> )	$y_2 \times 10^5$ (Mole fraction)	S (Equilibrium solubility) (g/L)	Experimental standard deviation, S( $\bar{y}$ ) $\times (10^5)$	Expanded uncertainty of mole fraction ( $10^5$ U)
308	120	769	0.393	0.0607	0.011	0.027
	150	817	0.542	0.0889	0.014	0.037
	180	849	0.697	0.1189	0.020	0.051
	210	875	1.079	0.1895	0.041	0.095
	240	896	1.200	0.2158	0.051	0.115
	270	914	1.603	0.2942	0.061	0.141
318	120	661	0.304	0.0403	0.012	0.026
	150	744	0.440	0.0657	0.021	0.046
	180	791	0.554	0.0879	0.012	0.034
	210	824	0.973	0.1610	0.015	0.052
	240	851	1.316	0.2248	0.010	0.063
	270	872	1.731	0.3031	0.073	0.165
328	120	509	0.203	0.0208	0.010	0.022
	150	656	0.345	0.0455	0.011	0.025
	180	725	0.455	0.0663	0.013	0.031
	210	769	0.770	0.1189	0.019	0.051
	240	802	1.490	0.2400	0.021	0.078
	270	829	1.886	0.3138	0.032	0.104
338	120	388	0.104	0.0081	0.001	0.005
	150	557	0.268	0.0300	0.002	0.013
	180	652	0.365	0.0478	0.011	0.028
	210	710	0.679	0.0969	0.028	0.064
	240	751	1.635	0.2466	0.021	0.084
	270	783	2.062	0.3242	0.025	0.104

<sup>a</sup> Standard uncertainty  $u$  is herein set to  $u(T) = \pm 0.1$  K and  $u(P) = \pm 1$  bar. The coverage factor,  $k = 2$  corresponds to a confidence level of approximately 95 %.

the solutes is approximately equal to one, the following equation can be used for calculating  $\varphi_2$  with each EoS (Coimbra et al., 2006):

$$RT \ln \varphi_i = -RT \ln Z + \int_V^{\infty} \left[ \left( \frac{\partial P}{\partial n_i} \right)_{T, V, n_j \neq n_i} - \frac{RT}{V} \right] dV \quad (6)$$

Various methods can be used to estimate the physicochemical properties of drug compounds such as  $T_c$ ,  $P_c$ ,  $P^{sub}$ , and  $V_s$ . In this study, Joback, Marrero and Pardillo, Grigoros, Fedors, Ambrose-Walton, and Lee-Kesler methods (Joback and Reid, 1987; Fedors, 1974; Poling et al., 2001) were used to calculate the critical properties. It should be noted that, using only a single EoS, the solubility of the compounds cannot be obtained.

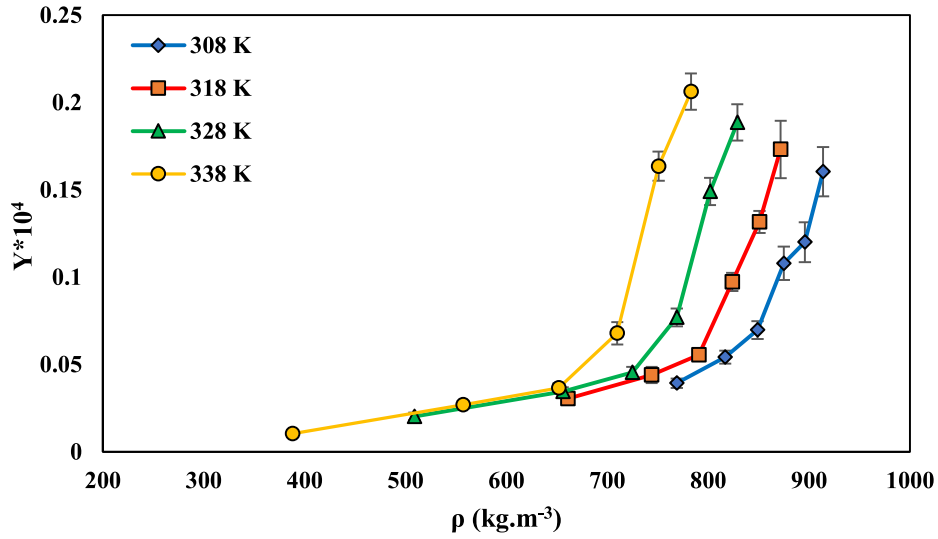


Fig. 2 The solubility of rivaroxaban in SC-CO<sub>2</sub> vs density of SC-CO<sub>2</sub> at different temperatures.

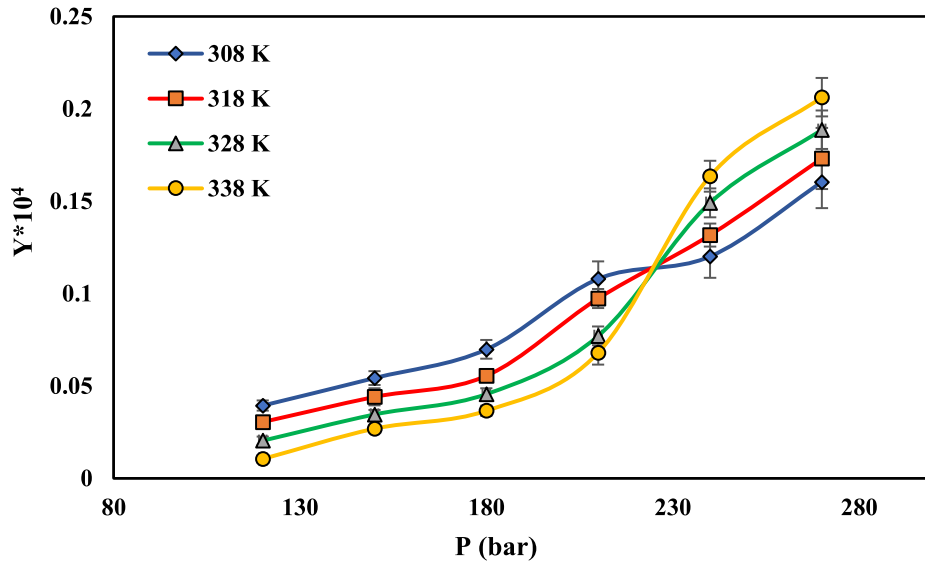


Fig. 3 The solubility of rivaroxaban in SC-CO<sub>2</sub> vs pressure at different temperatures.

Mixing rules help us to solve this problem. In this research, PR and SRK EoSs with vdW2 and CVD mixing rules were used. PR EoS is written as follows:

$$P = \frac{RT}{V-b} - \frac{a\alpha}{V^2 + 2bV - b^2} \quad (7)$$

Where  $P$ ,  $T$ ,  $V$  and  $R$  are pressure, temperature, molar volume and gas constant, respectively. The parameters  $a$  and  $b$  calculated as follows:

$$a = 0.45724 \frac{R^2 T_C^2}{P_C} \quad (8)$$

$$b = 0.07780 \frac{RT_C}{P_C} \quad (9)$$

$$\alpha = \left(1 + k \left(1 - T_r^{0.5}\right)\right)^2 \quad (10)$$

$$k = 0.37464 + 1.54226\omega - 0.26992\omega^2 \quad (11)$$

Soave-Redlich-Kwong (SRK) EoS is written as follows:

$$P = \frac{RT}{V-b} - \frac{a(T)}{V(V+b)} \quad (12)$$

$$a(T) = \frac{0.42748R^2 T_C^2}{P_C} \times \alpha(T_{r,\omega}) \quad (13)$$

$$\alpha(T_{r,\omega}) = [1 + m(1 - T_r^{0.5})]^2 \quad (14)$$

$$m = 0.480 + 1.574\omega - 0.176\omega^2 \quad (15)$$

$$b = \frac{0.08664RT_C}{P_C} \quad (16)$$

$\omega$  is acentric factor for each compound.



**Table 4** Statistical tools for the capability evaluation and verification of the used models.

Equation	Parameters	References
$AARD\% = \frac{100}{N} \sum_{i=1}^N \left  \frac{y_i^{calc} - y_i^{exp}}{y_i^{exp}} \right $	<ul style="list-style-type: none"> <li>• N is the number of data base.</li> <li>• <math>y_i^{calc}</math> is calculated values of the solute solubility</li> <li>• <math>y_i^{exp}</math> is experimental value of the solute solubility</li> </ul>	(Esmaeili et al., 2019)
$R_{adj} = \sqrt{R^2 - \left( \frac{Q(1-R^2)}{N-Q-1} \right)}$ $R^2 = 1 - \frac{SS_E}{SS_T}$	<ul style="list-style-type: none"> <li>• Q is the number of independent variables in each equation</li> <li>• <math>R^2</math> is the correlation coefficient</li> <li>• <math>SS_E</math> and <math>SS_T</math> is the error sum and total sum of squares</li> </ul>	(Sodeifian and Sajadian, 2019)
$F\text{-value} = \frac{\frac{SS_R}{Q}}{\frac{SS_E}{N-Q-1}} = \frac{MS_R}{MS_E}$	<ul style="list-style-type: none"> <li>• <math>SS_R</math> is the regression sum of squares</li> <li>• <math>MS_R</math> and <math>MS_E</math> is the mean square regression and residual</li> </ul>	(Ardestani et al., 2020)

**Table 5** Result of semi-empirical models for rivaroxaban solubility in SC-CO<sub>2</sub>.

Model	Chrastil	Bartle	Jafari Nejad	Jouyban	Sodeifian	Belghait
parameter						
$a_0$	9.508	15.912	-24.973	-13.986	-20.982	-168.862
$a_1$	-5246.281	-7612.323	0.002	-1.104	1.137	-0.265
$a_2$	-49.845	0.015	1.583E-6	1.182E-5	1.106	3.969e-5
$a_3$	—	—	1.812	3.232E-5	7.596e-4	6.705e-4
$a_4$	—	—	—	0.701	-0.017	0.068
$a_5$	—	—	—	2.962	-389.092	-8.536e-5
$a_6$	—	—	—	—	—	0.357
$a_7$	—	—	—	—	—	50314.666
AARD	25.201	24.828	13.788	12.463	14.297	19.188
Radj	0.959	0.960	0.921	0.969	0.923	0.936
F-value	90.285	91.603	44.410	90.54	45.266	—

vdW2 and CVD mixing rules are explained as below:

A: vdW2 mixing rule:

$$a_m = \sum_i \sum_j y_i y_j a_{ij} \quad (17)$$

$$b_m = \sum_i \sum_j y_i y_j b_{ij} \quad (18)$$

$$a_{ij} = \sqrt{a_{ii} a_{jj}} (1 - K_{ij}) \quad (19)$$

$$b_{ij} = \frac{b_i + b_j}{2} (1 - l_{ij}) \quad (20)$$

Where  $l_{ij}$  and  $K_{ij}$  are interaction parameters and given:

$$\hat{a}_i = \left[ \frac{\partial(na_m)}{\partial(n_i)} \right]_{T,P,n_j \neq i} = 2 \sum_{j=1}^N y_j a_{ij} \quad (21)$$

$$\hat{b}_i = \left[ \frac{\partial(nb_m)}{\partial(n_i)} \right]_{TP,n_j \neq i} = 2 \sum_{j=1}^N y_j b_{ij} \quad (22)$$

B: CVD mixing rule:

$$a = \sum_i \sum_j x_i x_j a_{ij} \left( \frac{b_m}{b_i} \right)^{M_{ij}} \quad (23)$$

$$b_m = \sum_i x_i b_i \quad (24)$$

$$a = \sqrt{a_i a_j} \quad (25)$$

$$b_{ij} = \sqrt{b_i b_j} \quad (26)$$

Where  $M_{ij}$  is the interaction parameter and given:

$$\begin{aligned} \hat{\partial}_i &= \left[ \frac{\partial(na_m)}{\partial(n_i)} \right]_{T,P,n_j \neq i} \\ &= 2 \sum_{j=1}^N \left( x_i a_{ij} \left( \frac{b_m}{b_{ij}} \right)^{M_{ij}} \right) \\ &\quad + \left( \frac{b_i}{b_m} - 1 \right) \left[ \sum_i \sum_j x_i x_j a_{ij} M_{ij} \left( \frac{b_m}{b_{ij}} \right)^{M_{ij}} \right] - a_m \end{aligned} \quad (27)$$

$$\hat{b}_i = \left[ \frac{\partial(nb_m)}{\partial(n_i)} \right]_{T,P,n_j \neq i} = 2 \sum_{j=1}^N x_j b_{ij} \quad (28)$$

Where  $M_{ij}$  is subjected to the following relations:

$$M_{ii} = M_{jj} = 1 \quad (29)$$

$$M_{ij} = M_{ji} \quad (30)$$

## 4. Results and discussion

### 4.1. Experimental data

In this study, the solubility of rivaroxaban in SC-CO<sub>2</sub> was investigated at various temperatures (308–338 K) and pressures (120–270 bar). Drug solubility in SC-CO<sub>2</sub> is given in

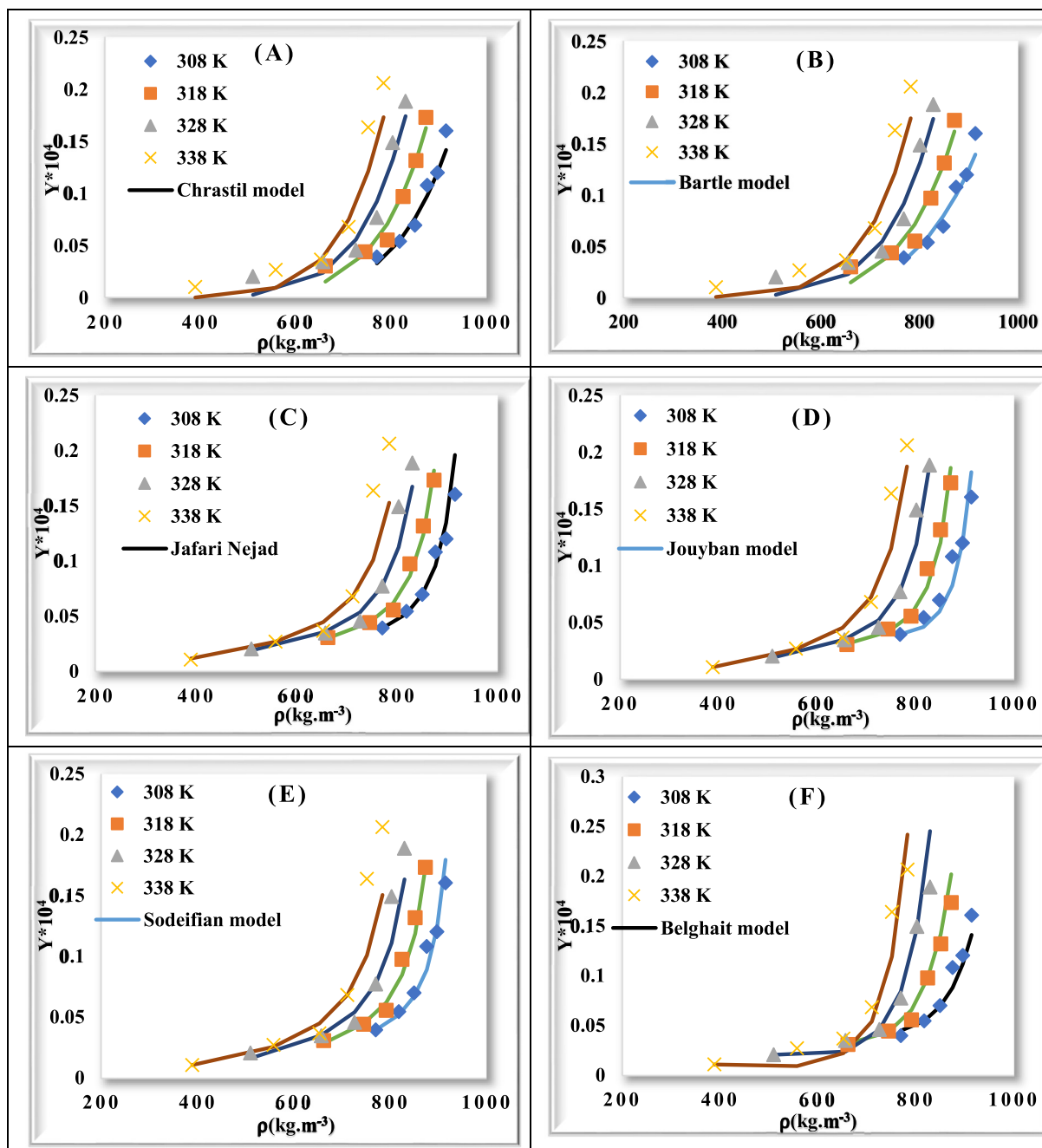


Fig. 4 Comparison of experimental (point) and calculated (line) values of rivaroxaban solubility.

Table 6 Approximated  $\Delta H_{total}$ ,  $\Delta H_{vap}$  and  $\Delta H_{sol}$  for rivaroxaban.

Compound	$\Delta H_{total} (\frac{kJ}{mol})^a$	$\Delta H_{vap} (\frac{kJ}{mol})^b$	$\Delta H_{sol} (\frac{kJ}{mol})^c$
Rivaroxaban	43.617	63.288	-19.671

<sup>a</sup>Obtained from the Chrastil model.

<sup>b</sup>Obtained from the Bartle model.

<sup>c</sup> $\Delta H_{sol} = \Delta H_{total} - \Delta H_{vap}$ .



**Table 7** The physicochemical properties of rivaroxaban.

Component	$T_b(K)$	$T_c(K)$	$P_c(bar)$	$\omega$	$V_s(\frac{cm^3}{mol})$	$T(K)$			
						308	318	328	338
						$P_{sub}(Pa)^f$			
Rivaroxaban	586.298 <sup>a</sup>	751.094 <sup>b</sup>	22.837 <sup>c</sup>	1.111 <sup>d</sup>	296.5 <sup>e</sup>	0.0047	0.0169	0.0557	0.1685
CO <sub>2</sub>	—	304.2	73.8	0.228	—	—	—	—	—

<sup>a</sup>Estimated by Marrero and Pardillo (Poling et al., 2001).

<sup>b</sup>Estimated by Joback (Poling et al., 2001).

<sup>c</sup>Estimated by Grigoros method (Poling et al., 2001).

<sup>d</sup>Estimated by Ambrose-Walton (Poling et al., 2001).

<sup>e</sup>Estimated by Fedors (Fedors, 1974).

<sup>f</sup>Estimated by lee-Kesler (Lee and Kesler, 1975).

**Table 8** Solubility correlation results of rivaroxaban for two different EoSs.

Model	Temperature	$M_{ij}$	$k_{ij}$	$l_{ij}$	$R_{adj}$	F-value	AARD%
PR EoS + vdW2	308	—	0.441	0.343	0.986	90.18	5.104
	318	—	0.504	0.443	0.989	1.141	8.012
	328	—	0.571	0.557	0.974	47.713	15.53
	338	—	0.650	0.701	0.966	35.528	14.732
SRK EoS + vdW2	308	—	0.466	0.369	0.986	88.662	5.314
	318	—	0.522	0.462	0.989	110.17	8.091
	328	—	0.527	0.410	0.755	4.317	15.117
	338	—	0.701	0.787	0.873	9.033	20.634
PR EoS + CVD	308	1.030	—	—	0.926	16.048	7.364
	318	1.092	—	—	0.8	5.447	15.826
	328	1.183	—	—	0.37	1.396	22.286
	338	1.339	—	—	0.842	-0.038	34.938
SRK EoS + CVD	308	1.040	—	—	0.825	6.308	9.729
	318	1.100	—	—	0.687	3.231	17.577
	328	1.207	—	—	0.575	0.378	31.97
	338	1.982	—	—	1.649	-0.828	71.861

**Table 9** Adjustable parameters of rivaroxaban.

Model	Interaction parameters			
	$K_{ij}$		$l_{ij}$	
	A	B	C	D
PR-vdW2	0.0069	-1.7001	0.0119	-3.3262
SRK-vdW2	0.0071	-1.7393	0.012	-3.3755

**Table 3.** All experiments were repeated triple to increase measurement accuracy. Using Spane-Wagner EoS (Span and Wagner, 1996), the density of CO<sub>2</sub> was estimated. Figs. 2 and 3 show the change in drug solubility with density and pressure, respectively. As shown in Fig. 2, the solubility of the drug increases with increasing density. Also, according to Fig. 3, the solubility of the drug increases with increasing pressure at a constant temperature, which is the result of increasing the density of CO<sub>2</sub> that increases the solubility of SC-CO<sub>2</sub> at higher pressures (Khimeche et al., 2007; Foster et al., 1991;

Sodeifian et al., 2021). Temperature has two different effects on solubility changes. There are graphs intersect at pressure of 225 bar. Before this pressure, the solubility decreases with increasing temperature and after this point, increases with increasing temperature. So at pressures less than 225 bar, with increasing temperature, solubility of drug decrease, and at pressures above 225 bar with increasing temperature the solubility increases. This type of solubility behavior is consistent with reports of other compounds by other researchers (Perrotin-Brunel et al., 2010; Sodeifian et al., 2018).

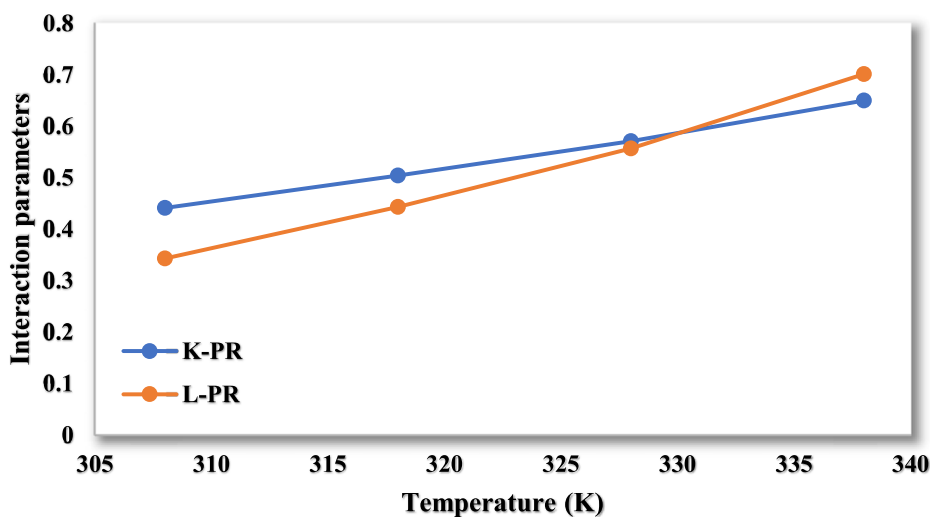


Fig. 5 The interaction parameters for the values of  $k_{ij}$  and  $l_{ij}$  in PR-vdW2.

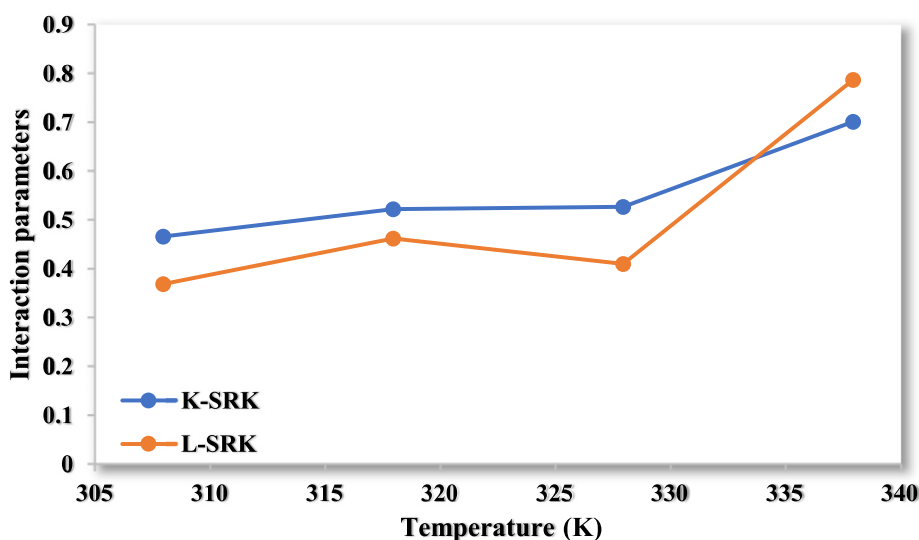


Fig. 6 The interaction parameters for the values of  $k_{ij}$  and  $l_{ij}$  in SRK-vdW2.

#### 4.2. Semi-empirical models

As stated before, six semi-empirical models were used to correlate solubility data of rivaroxaban in SC-CO<sub>2</sub>. Average absolute relative deviation (AARD), adjusted correlation coefficient ( $R_{adj}$ ) and F-value by MATLAB function (program) were used for the capability evaluation and verification of these models (Table 4). The results of these models are given in Table 5.

As shown in Table 5, considering the values of AARD for each model (Chrasil (AARD = 25.201); Bartle (AARD = 24.828), Jafari Nejad (AARD = 13.788), Jouyban (AARD = 12.463), Sodeifian (AARD = 14.297), and Belghait (AARD = 19.188)), Jouyban model has the lowest value of AARD and Chrastil model has the highest value of AARD. Therefore, the Jouyban model shows a better correlation with solubility data. Fig. 4 demonstrates the solubility correlation obtained from six models.

In terms of the number of adjustable parameters, the rivaroxaban solubility could be poorly correlated using models with three adjustable parameters, as compared to those with four, six and seven parameters, as shown in Table 5. In addition to AARD,  $R_{adj}$  was calculated to compare models of different numbers of independent variables. A model with more adjustable parameters can be considered superior to other models with less parameters that, in addition to AARD decrease,  $R_{adj}$  also increases. This can be seen for Jouyban model.

Elaborating on the results presented in this research, it can be reasoned that the energy term (coefficient of the temperature term ( $a_1 = \Delta H/R$ )) in the Chrastil and Bartle *et al.* models eased the determination of vaporization heat ( $\Delta H_{vap}$ ), total reaction heat ( $\Delta H_{total}$ ), and solvation heat ( $\Delta H_{sol}$ ) of the considered drug-CO<sub>2</sub> systems based on the regressed energy parameters. Indeed, the solvation heat ( $\Delta H_{sol}$ ) was defined as the difference between  $\Delta H_{vap}$  (Bartle *et al.* model) and  $\Delta H_{total}$

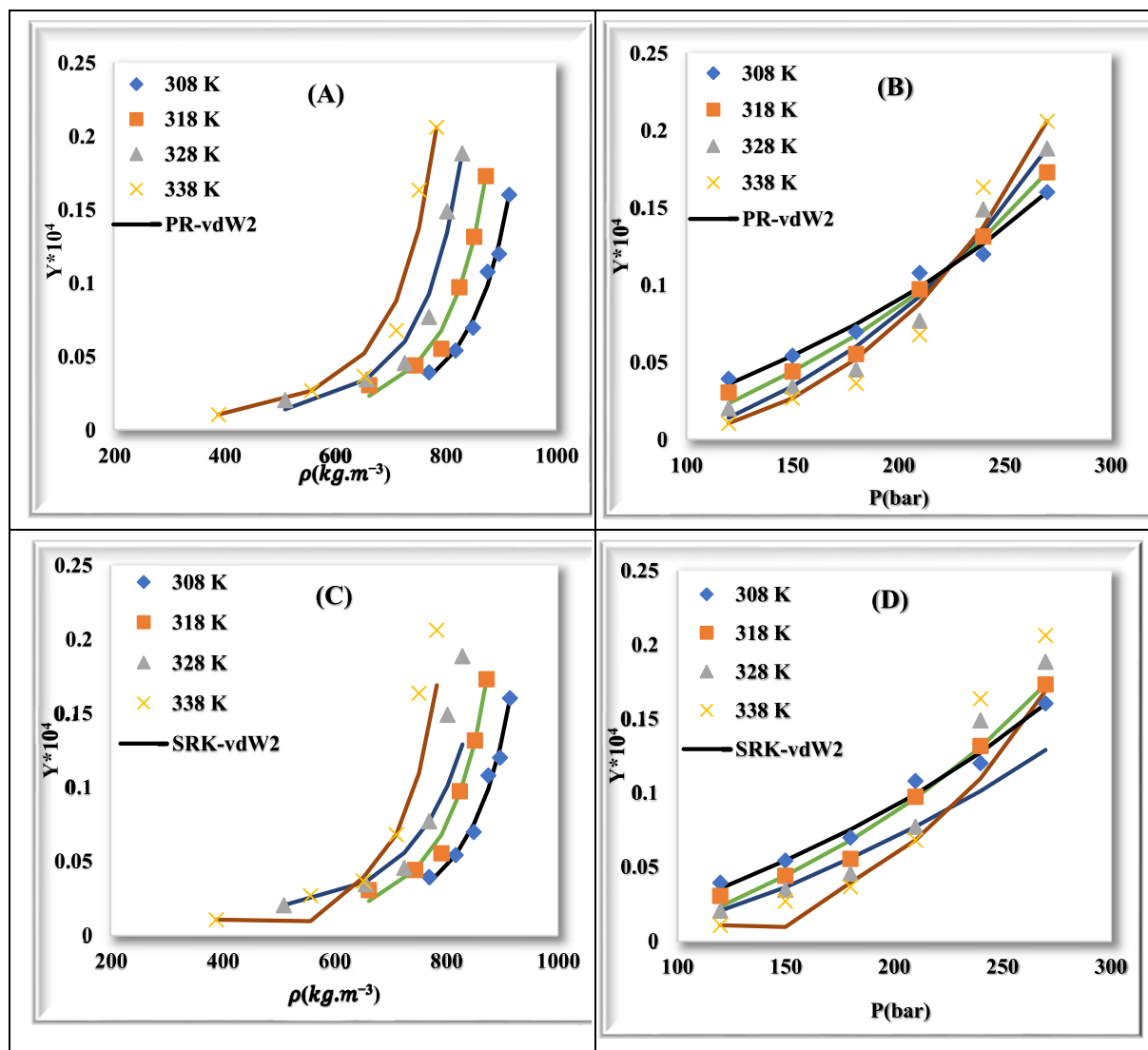


**Fig. 7** Comparison of experimental (point) and calculated (line) solubility of rivaroxaban at various temperatures. (a) & (b): PR-vdW2, (c) & (d): SRK-vdW2, (e) & (f): PR-CVD, and (g) & (h): SRK-CVD.

(Chrastil's model). According to Table 6, wherein enthalpy of dissolution of rivaroxaban in SC-CO<sub>2</sub> is presented, the corresponding values of  $\Delta H_{\text{total}}$  and  $\Delta H_{\text{vap}}$  to the Chrastil and Bartle *et al.* models were 43.617 and 63.288 kJ.mol<sup>-1</sup>, respectively. Given the endothermic and exothermic natures of vaporization and solvation processes, respectively, the value of vaporization heat was observed to be larger than the total heat. Representing the difference between  $\Delta H_{\text{vap}}$  and  $\Delta H_{\text{total}}$ , the value of  $\Delta H_{\text{sol}}$  was evaluated as -19.671 kJ.mol<sup>-1</sup>.

#### 4.3. Solubility correlation by EoS based model

Two mixing rules (vdW2 and CVD) were used to estimate the parameters of PR and SRK EoSs. The physicochemical properties of rivaroxaban were calculated with Ambrose, Joback, Marrero and Pardillo, Grigoros, Fedors and Lee-Kesler methods and shown in Table 7.

Table 8 shows the results two EoSs (PR and SRK) with two mixing rules (vdW2 and CVD). Parameters  $k_{ij}$  and  $l_{ij}$  were cal-

culated for vdW2 mixing rule and parameters  $M_{ij}$  were calculated for CVD mixing rule. In addition to the above, the value of the 123 parameters for each of the EoS with two mixing rules are shown in Table 8. As shown in Table 8, the lowest AARD are for PR EoS + vdW2 (AARD% = 5.104, T = 308 K), SRK EoS + vdW2 (AARD% = 5.314, T = 308 K), PR EoS + CVD (AARD% = 7.364, T = 308 K), and SRK EoS + CVD (AARD% = 9.729, T = 308 K) were obtained, respectively. In all four cases, the value of AARD generally decreased by decreasing the temperature.

Parameters  $k_{ij}$  and  $l_{ij}$  for vdW2 are calculated as follows:

$$k_{ij} = AT + B \quad (31)$$

$$l_{ij} = CT + D \quad (32)$$

The values A, B, C, and D for  $k_{ij}$  and  $l_{ij}$  were calculated with data in Table 8 and linear regression fitting results (Figs. 5 and 6 for PR and SRK, respectively) are shown in Table 9.

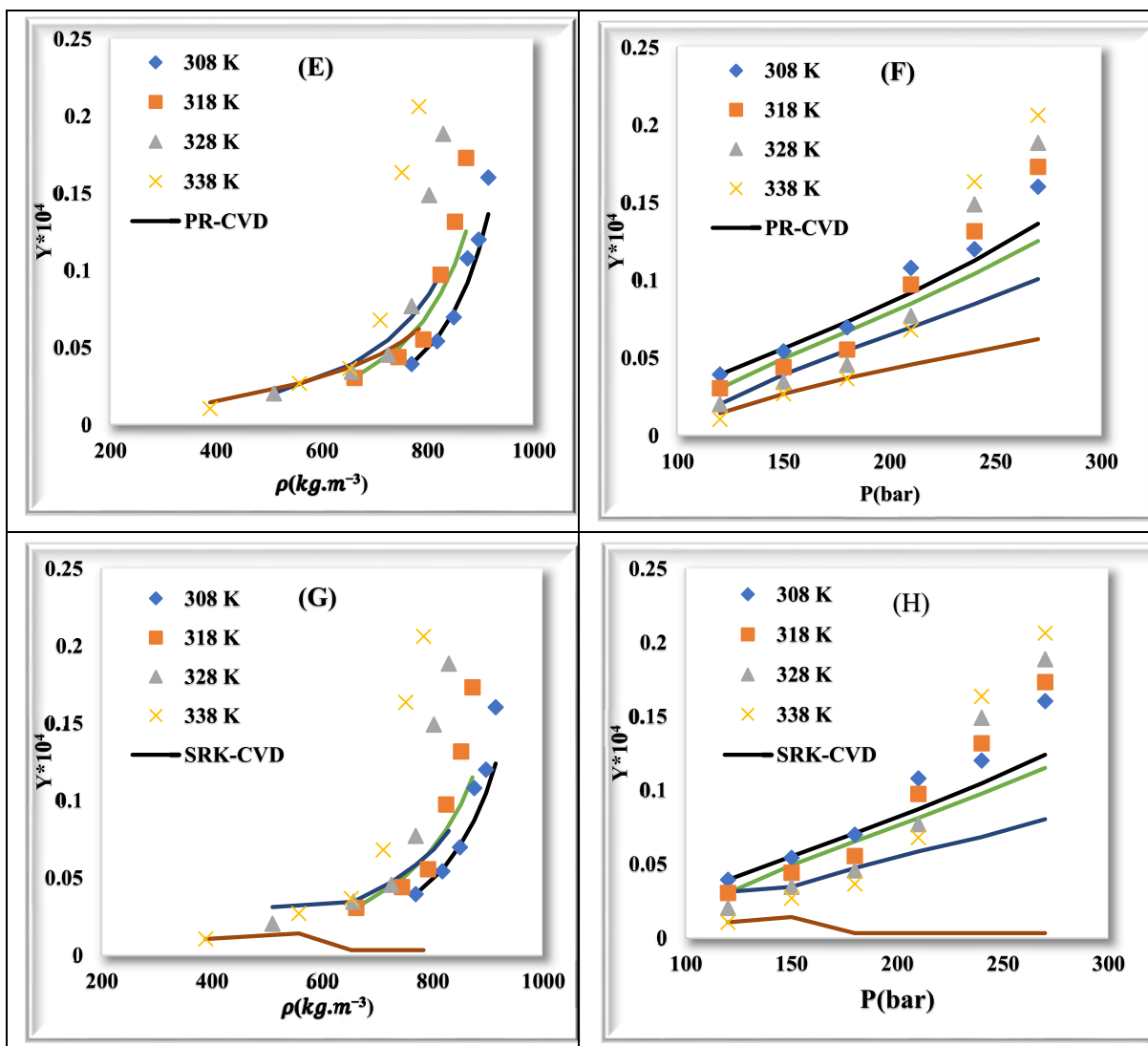


Fig. 7 (continued)

Fig. 7 shows plots of experimental data (point) and calculated values (line) for rivaroxaban drug with PR-vdW2 (a & b), SRK-vdW2 (c & d), PR-CVD (e & f), and SRK-CVD (g & h) at various temperatures relative to density and pressure, respectively. The correlation between experimental data and calculated values in different modes is well shown.

## 5. Conclusion

The solubility of rivaroxaban was determined at various temperatures and pressures in SC-CO<sub>2</sub> for the first time. The range of solubility of rivaroxaban was between 0.0104 and 0.2062 ( $\times 10^{-4}$ ) (in mole fraction). Maximum solubility of rivaroxaban at  $T = 338$  K and  $P = 270$  bar was  $0.2062 \times 10^{-4}$  (in mole fraction). Six semi-empirical models were used to examine the correlation of experimental data. Among the used models, the best performance was obtained for Jouyban model (AARD% = 12.4635), and the lowest was for Chrastil model (AARD% = 25.201). Then, two EoSs (PR and SRK) with vdW2 and CVD mixing rules were used to examine the correlation of sol-

ubility data. The best performance was obtained with PR + vdW2 (AARD% = 5.104 at 308 K). In both cases of semi-empirical models and EoSs, the values of  $R_{adj}$ , F-value, and AARD% were reported. Also, the amount of vaporization and total enthalpies were calculated by Bartle and Chrastil models. Using solubility data, important information can be obtained about the fabrication of micro/nano-scale particles using SCF to be used in the medical and pharmaceutical industries.

## Declaration of Competing Interest

The authors declare that they have no known competing financial interests or personal relationships that could have appeared to influence the work reported in this paper.

## Acknowledgement

The authors would like to thank of the deputy of research, University of Kashan, under Grant Number (#Pajoothaneh 1401/19) for supporting this valuable project. Also, researchers

would like to thank Parsian drug Company (Tehran), especially, Drs. Shojaei and Yosoufian, for providing the required drug API.

## Appendix A. Supplementary material

Supplementary data to this article can be found online at <https://doi.org/10.1016/j.arabjc.2022.104421>.

## References

- Adachi, Y., Lu, B.-C.-Y., 1983. Supercritical fluid extraction with carbon dioxide and ethylene. *Fluid Phase Equilib.* 14, 147–156. [https://doi.org/10.1016/0378-3812\(83\)80120-4](https://doi.org/10.1016/0378-3812(83)80120-4).
- Ardestani, N.S., Majd, N.Y., Amani, M., 2020. Experimental measurement and thermodynamic modeling of capecitabine (an anti-cancer drug) solubility in supercritical carbon dioxide in a ternary system: effect of different cosolvents. *J. Chem. Eng. Data* 65, 4762–4779. <https://doi.org/10.1021/acs.jced.0c00183>.
- Aredo, V., Bittencourt, G.M., Pallone, E.M.de J.A., et al, 2021. Formation of edible oil-loaded beeswax microparticles using PGSS – Particles from Gas-Saturated Solutions. *J. Supercritical Fluids* 169. <https://doi.org/10.1016/j.supflu.2020.105106> 105106.
- Asgarpour Khansary, M., Amiri, F., Hosseini, A., et al, 2015. Representing solute solubility in supercritical carbon dioxide: a novel empirical model. *Chem. Eng. Res. Des.* 93, 355–365. <https://doi.org/10.1016/j.cherd.2014.05.004>.
- Banchero, M., 2021. Supercritical carbon dioxide as a green alternative to achieve drug complexation with cyclodextrins. *Pharmaceuticals* 14, 562. <https://doi.org/10.3390/ph14060562>.
- Bartle, K.D., Clifford, A.A., Jafar, S.A., Shilstone, G.F., 1991. Solubilities of solids and liquids of low volatility in supercritical carbon dioxide. *J. Phys. Chem. Ref. Data* 20, 713–756. <https://doi.org/10.1063/1.555893>.
- Belghait, A., Si-Moussa, C., Laidi, M., Hanini, S., 2018. Semi-empirical correlation of solid solute solubility in supercritical carbon dioxide: comparative study and proposition of a novel density-based model. *C. R. Chim.* 21, 494–513. <https://doi.org/10.1016/j.crci.2018.02.006>.
- Bian, X.-Q., Li, J., Chen, J., et al, 2015. A combined model for the solubility of different compounds in supercritical carbon dioxide. *Chem. Eng. Res. Des.* 104, 416–428. <https://doi.org/10.1016/j.cherd.2015.08.028>.
- Bian, X.-Q., Zhang, Q., Du, Z.-M., et al, 2016. A five-parameter empirical model for correlating the solubility of solid compounds in supercritical carbon dioxide. *Fluid Phase Equilib.* 411, 74–80. <https://doi.org/10.1016/j.fluid.2015.12.017>.
- Brunner, G., 2015. Supercritical process technology related to energy and future directions – An introduction. *J. Supercritical Fluids* 96, 11–20. <https://doi.org/10.1016/j.supflu.2014.09.008>.
- Chen, B.-Q., Kankala, R.K., Wang, S.-B., Chen, A.-Z., 2018. Continuous nanonization of lonidamine by modified-rapid expansion of supercritical solution process. *J. Supercritical Fluids* 133, 486–493. <https://doi.org/10.1016/j.supflu.2017.11.016>.
- Chen, C.-T., Lee, C.-A., Tang, M., Chen, Y.-P., 2017. Experimental investigation for the solubility and micronization of pyridin-4-amine in supercritical carbon dioxide. *J. CO<sub>2</sub> Util.* 18, 173–180. <https://doi.org/10.1016/j.jcou.2017.01.020>.
- Ciou, J.-M., Wang, B.-C., Su, C.-S., et al, 2018. Measurement of solid solubility of warfarin in supercritical carbon dioxide and recrystallization study using supercritical antisolvent process. *Adv. Powder Technol.* 29, 479–487. <https://doi.org/10.1016/j.apt.2017.12.005>.
- Coelho, J.A.P., Filipe, R.M., Naydenova, G.P., et al, 2016. Semi-empirical models and a cubic equation of state for correlation of solids solubility in scCO<sub>2</sub>: dyes and calix[4]arenes as illustrative examples. *Fluid Phase Equilib.* 426, 37–46. <https://doi.org/10.1016/j.fluid.2016.01.026>.
- Cohen, A.T., Spiro, T.E., Büller, H.R., et al, 2011. Extended-duration rivaroxaban thromboprophylaxis in acutely ill medical patients: MAGELLAN study protocol. *J. Thromb. Thrombolysis* 31, 407–416. <https://doi.org/10.1007/s11239-011-0549-x>.
- Coimbra, P., Duarte, C.M.M., de Sousa, H.C., 2006. Cubic equation-of-state correlation of the solubility of some anti-inflammatory drugs in supercritical carbon dioxide. *Fluid Phase Equilib.* 239, 188–199. <https://doi.org/10.1016/j.fluid.2005.11.028>.
- Douxflis, J., Mullier, F., Loosen, C., et al, 2012. Assessment of the impact of rivaroxaban on coagulation assays: Laboratory recommendations for the monitoring of rivaroxaban and review of the literature. *Thromb. Res.* 130, 956–966. <https://doi.org/10.1016/j.thromres.2012.09.004>.
- Esmaeili, S., Sarma, H., Harding, T., Maini, B., 2019. A data-driven model for predicting the effect of temperature on oil-water relative permeability. *Fuel* 236, 264–277. <https://doi.org/10.1016/j.fuel.2018.08.109>.
- Esmaeilzadeh, F., Asadi, H., Lashkarbolooki, M., 2009. Calculation of the solid solubilities in supercritical carbon dioxide using a new Gex mixing rule. *J. Supercritical Fluids* 51, 148–158. <https://doi.org/10.1016/j.supflu.2009.08.005>.
- Farrokh-Nia, A.H., Moddarras, H., Mohsen-Nia, M., 2008. A three-parameter cubic equation of state for prediction of thermodynamic properties of fluids. *J. Chem. Thermodyn.* 40, 84–95. <https://doi.org/10.1016/j.jct.2007.05.012>.
- Fedors, R.F., 1974. A method for estimating both the solubility parameters and molar volumes of liquids. *Polym. Eng. Sci.* 14, 147–154. <https://doi.org/10.1002/pen.760140211>.
- Foster, N.R., Gurdial, G.S., Yun, J.S.L., et al, 1991. Significance of the crossover pressure in solid-supercritical fluid phase equilibria. *Ind. Eng. Chem. Res.* 30, 1955–1964. <https://doi.org/10.1021/ie00056a044>.
- Garlapati, C., Madras, G., 2009. Solubilities of solids in supercritical fluids using dimensionally consistent modified solvate complex models. *Fluid Phase Equilib.* 283, 97–101. <https://doi.org/10.1016/j.fluid.2009.05.013>.
- Hazaveie, S.M., Sodeifian, G., Sajadian, S.A., 2020. Measurement and thermodynamic modeling of solubility of Tamsulosin drug (anti cancer and anti-prostatic tumor activity) in supercritical carbon dioxide. *J. Supercritical Fluids* 163. [https://doi.org/10.1016/j-supflu.2020.104875](https://doi.org/10.1016/j.supflu.2020.104875) 104875.
- Hozhabr, S.B., Mazloumi, S.H., Sargolzaei, J., 2014. Correlation of solute solubility in supercritical carbon dioxide using a new empirical equation. *Chem. Eng. Res. Des.* 92, 2734–2739. <https://doi.org/10.1016/j.cherd.2014.01.026>.
- Huang, C.-Y., Lee, L.-S., Su, C.-S., 2013. Correlation of solid solubilities of pharmaceutical compounds in supercritical carbon dioxide with solution model approach. *J. Taiwan Inst. Chem. Eng.* 44, 349–358. <https://doi.org/10.1016/j.jtice.2012.12.004>.
- Jafari Nejad, S.h., Abolghasemi, H., Moosavian, M.A., Maragheh, M. G., 2010. Prediction of solute solubility in supercritical carbon dioxide: a novel semi-empirical model. *Chem. Eng. Res. Des.* 88, 893–898. <https://doi.org/10.1016/j.cherd.2009.12.006>.
- Jafari, D., Yarnezhad, I., Nowee, S.M., Baghban, S.H.N., 2015. Gas-Antisolvent (GAS) crystallization of aspirin using supercritical carbon dioxide: experimental study and characterization. *Ind. Eng. Chem. Res.* 54, 3685–3696. <https://doi.org/10.1021/ie5046445>.
- Jaubert, J.-N., Privat, R., 2010. Relationship between the binary interaction parameters (kij) of the Peng-Robinson and those of the Soave-Redlich-Kwong equations of state: Application to the definition of the PR2SRK model. *Fluid Phase Equilib.* 295, 26–37. <https://doi.org/10.1016/j.fluid.2010.03.037>.
- Joback, K.G., Reid, R.C., 1987. Estimation of pure-component properties from group-contributions. *Chem. Eng. Commun.* 57, 233–243. <https://doi.org/10.1080/00986448708960487>.



- Jouyban, A., Chan, H.-K., Foster, N.R., 2002. Mathematical representation of solute solubility in supercritical carbon dioxide using empirical expressions. *J. Supercritical Fluids* 24, 19–35. [https://doi.org/10.1016/S0896-8446\(02\)00015-3](https://doi.org/10.1016/S0896-8446(02)00015-3).
- Jouyban, A., Khoubnasabjafari, M., Acree, W.E., 2005. Mathematical representation of solute solubility in binary mixture of supercritical fluids by the Jouyban-Acree model. 3.
- Jouyban, A., Khoubnasabjafari, M., Chan, H.-K., 2005. Modeling the entrainer effects on solubility of solutes in supercritical carbon dioxide. *Chem. Pharm. Bull.* 53, 290–295. <https://doi.org/10.1248/cpb.53.290>.
- Khimeche, K., Alessi, P., Kikic, I., Dahmani, A., 2007. Solubility of diamines in supercritical carbon dioxide Experimental determination and correlation. 10.
- Kiran, E., 2016. Supercritical fluids and polymers – The year in review – 2014. *J. Supercritical Fluids* 110, 126–153. <https://doi.org/10.1016/j.supflu.2015.11.011>.
- Kodama, T., Honda, M., Takemura, R., et al, 2018. Effect of the Z-isomer content on nanoparticle production of lycopene using solution-enhanced dispersion by supercritical fluids (SEDS). *J. Supercritical Fluids* 133, 291–296. <https://doi.org/10.1016/j.supflu.2017.10.028>.
- Lee, B.I., Kesler, M.G., 1975. A generalized thermodynamic correlation based on three-parameter corresponding states. *AIChE J.* 21, 510–527. <https://doi.org/10.1002/aic.690210313>.
- Lee, W.J., Tan, C.P., Sulaiman, R., et al, 2018. Microencapsulation of red palm oil as an oil-in-water emulsion with supercritical carbon dioxide solution-enhanced dispersion. *J. Food Eng.* 222, 100–109. <https://doi.org/10.1016/j.foodeng.2017.11.011>.
- Lee, W.J., Tan, C.P., Sulaiman, R., et al, 2020. Storage stability and degradation kinetics of bioactive compounds in red palm oil microcapsules produced with solution-enhanced dispersion by supercritical carbon dioxide: a comparison with the spray-drying method. *Food Chem.* 304,. <https://doi.org/10.1016/j.foodchem.2019.125427>.
- Mega, J.L., Braunwald, E., Wiviott, S.D., et al, 2012. Rivaroxaban in patients with a recent acute coronary syndrome. *N. Engl. J. Med.* 366, 9–19. <https://doi.org/10.1056/NEJMoa1112277>.
- Montes, A., Merino, R., De los Santos, D.M., et al, 2017. Micronization of vanillin by rapid expansion of supercritical solutions process. *J. CO<sub>2</sub> Util.* 21, 169–176. <https://doi.org/10.1016/j.jcou.2017.07.009>.
- Mueck, W., Lensing, A.W.A., Agnelli, G., et al, 2011. Rivaroxaban: population pharmacokinetic analyses in patients treated for acute deep-vein thrombosis and exposure simulations in patients with atrial fibrillation treated for stroke prevention. *Clin. Pharmacokinet.* 50, 675–686. <https://doi.org/10.2165/11595320-000000000-00000>.
- Nasri, L., 2018. Modified Wilson's model for correlating solubilities in supercritical fluids of some polycyclic aromatic solutes. *Polycyclic Aromat. Compd.* 38, 244–256. <https://doi.org/10.1080/10406638.2016.1200636>.
- Perrotin-Brunel, H., Perez, P.C., Witkamp, G.-J., Peters, C.J., 2010. Solubility of 9-tetrahydrocannabinol in supercritical carbon dioxide. *Experiments Modeling* 5.
- Poling, B.E., Prausnitz, J.M., O'Connell, J.P., 2001. *The properties of gases and liquids*. McGraw-Hill, New York.
- Razmimanesh, F., Sodeifian, G., Sajadian, S.A., 2021. An investigation into Sunitinib malate nanoparticle production by US-RESOLV method: effect of type of polymer on dissolution rate and particle size distribution. *J. Supercritical Fluids* 170,. <https://doi.org/10.1016/j.supflu.2021.105163>.
- Reddy, T.A., Garlapati, C., 2019. Dimensionless empirical model to correlate pharmaceutical compound solubility in supercritical carbon dioxide. *Chem. Eng. Technol.* 42, 2621–2630. <https://doi.org/10.1002/ceat.201900283>.
- Sang, J., Wang, H., Jin, J., Meng, H., 2017. Comparison and modelling of rutin solubility in supercritical carbon dioxide and subcritical 1,1,1,2-tetrafluoroethane. *J. CO<sub>2</sub> Util.* 21, 1–8. <https://doi.org/10.1016/j.jcou.2017.06.006>.
- Shamsipur M, Karami AR, Yamini Y, Sharghi H (2004) Solubilities of some 1-hydroxy-9,10-anthraquinone derivatives in supercritical carbon dioxide. 7.
- Sheikhi-Kouhsar, M., Bagheri, H., Raeissi, S., 2015. Modeling of ionic liquid + polar solvent mixture molar volumes using a generalized volume translation on the Peng-Robinson equation of state. *Fluid Phase Equilib.* 395, 51–57. <https://doi.org/10.1016/j.fluid.2015.03.005>.
- Sim Yeoh, H., Hean Chong, G., Mohd Azahan, N., et al, 2013. Solubility measurement method and mathematical modeling in supercritical fluids. *EJ* 17, 67–78. <https://doi.org/10.4186/ej.2013.17.3.67>.
- Si-Moussa, C., Belghait, A., Khaouane, L., et al, 2017. Novel density-based model for the correlation of solid drugs solubility in supercritical carbon dioxide. *C. R. Chim.* 20, 559–572. <https://doi.org/10.1016/j.crci.2016.09.009>.
- Sodeifian, G., Sajadian, S.A., Ardestani, N.S., 2017. Determination of solubility of Aprepitant (an antiemetic drug for chemotherapy) in supercritical carbon dioxide: empirical and thermodynamic models. *J. Supercritical Fluids* 128, 102–111. <https://doi.org/10.1016/j.supflu.2017.05.019>.
- Sodeifian, G., Razmimanesh, F., Sajadian, S.A., Soltani Panah, H., 2018. Solubility measurement of an antihistamine drug (Loratadine) in supercritical carbon dioxide: assessment of qCPA and PCP-SAFT equations of state. *Fluid Phase Equilib.* 472, 147–159. <https://doi.org/10.1016/j.fluid.2018.05.018>.
- Sodeifian, G., Saadati Ardestani, N., Sajadian, S.A., 2019. Solubility measurement of a pigment (Phthalocyanine green) in supercritical carbon dioxide: Experimental correlations and thermodynamic modeling. *Fluid Phase Equilib.* 494, 61–73. <https://doi.org/10.1016/j.fluid.2019.04.024>.
- Sodeifian, G., Razmimanesh, F., Sajadian, S.A., Hazaveie, S.M., 2020. Experimental data and thermodynamic modeling of solubility of Sorafenib tosylate, as an anti-cancer drug, in supercritical carbon dioxide: Evaluation of Wong-Sandler mixing rule. *J. Chem. Thermodyn.* 142,. <https://doi.org/10.1016/j.jct.2019.105998>.
- Sodeifian, G., Sajadian, S.A., 2019. Experimental measurement of solubilities of sertraline hydrochloride in supercritical carbon dioxide with/without menthol: data correlation. *J. Supercritical Fluids* 149, 79–87. <https://doi.org/10.1016/j.supflu.2019.03.020>.
- Sodeifian, G., Sajadian, S.A., Saadati Ardestani, N., 2016. Evaluation of the response surface and hybrid artificial neural network-genetic algorithm methodologies to determine extraction yield of *Ferulago angulata* through supercritical fluid. *J. Taiwan Inst. Chem. Eng.* 60, 165–173. <https://doi.org/10.1016/j.jtice.2015.11.003>.
- Sodeifian, G., Sajadian, S.A., Honarvar, B., 2018. Mathematical modelling for extraction of oil from *Dracocephalum kotschy* seeds in supercritical carbon dioxide. *Nat. Prod. Res.* 32, 795–803. <https://doi.org/10.1080/14786419.2017.1361954>.
- Sodeifian, G., Razmimanesh, F., Sajadian, S.A., 2019. Solubility measurement of a chemotherapeutic agent (Imatinib mesylate) in supercritical carbon dioxide: assessment of new empirical model. *J. Supercritical Fluids* 146, 89–99. <https://doi.org/10.1016/j.supflu.2019.01.006>.
- Sodeifian, G., Saadati Ardestani, N., Sajadian, S.A., et al, 2020. Prediction of solubility of sodium valproate in supercritical carbon dioxide: experimental study and thermodynamic modeling. *J. Chem. Eng. Data* 65, 1747–1760. <https://doi.org/10.1021/acs.jced.9b01069>.
- Sodeifian, G., Razmimanesh, F., Sajadian, S.A., 2020. Prediction of solubility of sunitinib malate (an anti-cancer drug) in supercritical carbon dioxide (SC-CO<sub>2</sub>): experimental correlations and thermodynamic modeling. *J. Mol. Liq.* 297,. <https://doi.org/10.1016/j.molliq.2019.111740>.
- Sodeifian, G., Sajadian, S.A., Derakhsheshpour, R., 2020. Experimental measurement and thermodynamic modeling of Lansoprazole

- solubility in supercritical carbon dioxide: application of SAFT-VR EoS. *Fluid Phase Equilib.* 507,. <https://doi.org/10.1016/j.fluid.2019.112422> 112422.
- Sodeifian, G., Nasri, L., Razmimanesh, F., Abadian, M., 2021. Measuring and modeling the solubility of an antihypertensive drug (losartan potassium, Cozaar) in supercritical carbon dioxide. *J. Mol. Liq.* 331,. <https://doi.org/10.1016/j.molliq.2021.115745> 115745.
- Sodeifian, G., Garlapati, C., Razmimanesh, F., Sodeifian, F., 2021. The solubility of Sulfabenzamide (an antibacterial drug) in supercritical carbon dioxide: evaluation of a new thermodynamic model. *J. Mol. Liq.* 335,. <https://doi.org/10.1016/j.molliq.2021.116446> 116446.
- Sodeifian, G., Garlapati, C., Razmimanesh, F., Sodeifian, F., 2021. Solubility of Amlodipine Besylate (Calcium Channel Blocker Drug) in supercritical carbon dioxide: measurement and correlations. *J. Chem. Eng. Data* 66, 1119–1131. <https://doi.org/10.1021/acs.jced.0c00913>.
- Sodeifian, G., Sajadian, S.A., 2017. Investigation of essential oil extraction and antioxidant activity of *Echinophora platyloba* DC. using supercritical carbon dioxide. *J. Supercritical Fluids* 121, 52–62. <https://doi.org/10.1016/j.supflu.2016.11.014>.
- Sodeifian, G., Razmimanesh, F., Saadati Ardestani, N., Sajadian, S. A., 2020. Experimental data and thermodynamic modeling of solubility of Azathioprine, as an immunosuppressive and anti-cancer drug, in supercritical carbon dioxide. *J. Mol. Liq.* 299,. <https://doi.org/10.1016/j.molliq.2019.112179> 112179.
- Span, R., Wagner, W., 1996. A new equation of state for carbon dioxide covering the fluid region from the triple-point temperature to 1100 K at pressures up to 800 MPa. *J. Phys. Chem. Ref. Data* 25, 1509–1596. <https://doi.org/10.1063/1.555991>.
- Sparks, D.L., Hernandez, R., Estévez, L.A., 2008. Evaluation of density-based models for the solubility of solids in supercritical carbon dioxide and formulation of a new model. *Chem. Eng. Sci.* 63, 4292–4301. <https://doi.org/10.1016/j.ces.2008.05.031>.
- Sridar, R., Bhowal, A., Garlapati, C., 2013. A new model for the solubility of dye compounds in supercritical carbon dioxide. *Thermochim Acta* 561, 91–97. <https://doi.org/10.1016/j.tca.2013.03.029>.
- Tabernero, A., Martín del Valle, E.M., Galán, M.A., 2012. Supercritical fluids for pharmaceutical particle engineering: methods, basic fundamentals and modelling. *Chem. Eng. Process. Process Intensif.* 60, 9–25. <https://doi.org/10.1016/j.ccep.2012.06.004>.
- Tokunaga, S., Ono, K., Ito, S., et al, 2021. Microencapsulation of drug with enteric polymer Eudragit L100 for controlled release using the particles from gas saturated solutions (PGSS) process. *J. Supercritical Fluids* 167,. <https://doi.org/10.1016/j.supflu.2020.105044> 105044.
- Yazdizadeh, M., Eslamimanesh, A., Esmailzadeh, F., 2011. Thermodynamic modeling of solubilities of various solid compounds in supercritical carbon dioxide: effects of equations of state and mixing rules. *J. Supercritical Fluids* 55, 861–875. <https://doi.org/10.1016/j.supflu.2010.10.019>.
- Yazdizadeh, M., Eslamimanesh, A., Esmailzadeh, F., 2012. Applications of cubic equations of state for determination of the solubilities of industrial solid compounds in supercritical carbon dioxide: a comparative study. *Chem. Eng. Sci.* 71, 283–299. <https://doi.org/10.1016/j.ces.2011.10.055>.